



ELSEVIER

Biochimica et Biophysica Acta 1388 (1998) 143–153

BIOCHIMICA ET BIOPHYSICA ACTA

BBA

Picosecond tryptophan fluorescence of membrane-bound prothrombin fragment 1¹

Martin Hof^{a, b, *}^a *J. Heyrovský Institute of Physical Chemistry, Academy of Sciences of the Czech Republic, Dolejškova 3, 18223 Prague 8, Czech Republic*^b *Institute for Physical Chemistry, University of Würzburg, Am Hubland, 97074 Würzburg, Germany*

Received 4 May 1998; revised 10 July 1998; accepted 28 July 1998

Abstract

The wavelength-dependent tryptophan (Trp) fluorescence decays of Ca-prothrombin fragment 1 (Ca-BF1), which contains three tryptophan residues, in the presence of pure phosphatidylcholine (PC) small unilamellar vesicles (SUV) and PC-SUV containing either 25% phosphatidyl-L-serine (PS), and 25% or 40% phosphatidylglycerol (PG) are characterized, using fluorescence lifetime distribution, conventional multiexponential, and global analysis. In analogy to previous investigations on apo- and Ca-BF1 (M. Hof, G.R. Fleming, V. Fidler, *Proteins Struct. Func. Genet.* 24 (1996) 485–494), the analysis resulted in a five exponential decay model in all investigated systems, where the five fluorescence lifetimes (e.g. 0.04 ± 0.02 ns (component A), 0.24 ± 0.02 ns (B), 0.66 ± 0.03 ns (C), 2.4 ± 0.3 ns (D), and 5.4 ± 0.4 ns (E) for Ca-BF1 in the presence of PC-SUV) are wavelength-independent. The fluorescence lifetimes and the corresponding amplitudes of the ‘Gla-Trp’ (components D and E) and of the two ‘kringle-Trp’ (components B, C, and D) remain unchanged when bound to the PS-containing vesicles. Saturation binding to PG-containing membranes leads to a prolongation of the Gla component E from 5.3 in solution to 7.5 ns, indicating a change in the Gla-domain conformation. The results represent the first experimental evidence of a lipid-specific conformational change in the N-terminal ‘Gla domain’ of a vitamin K-dependent protein. © 1998 Elsevier Science B.V. All rights reserved.

Keywords: Tryptophan fluorescence; Lifetimes distribution analysis; Blood coagulation; Factor II; γ -Carboxyglutamic acid domain; Phosphatidylserine; Phosphatidylglycerol

1. Introduction

Prothrombin is the substrate of the ‘prothrombinase’ complex, which consists of the serine protease factor Xa, the protein co-factor Va, calcium ions and anionic phospholipid surfaces [2]. Membranes composed of certain acidic phospholipids [3–5] increase

the turnover number of the prothrombin proteolysis by roughly a thousandfold relative to the rate of catalysis in the absence of phospholipid surfaces. A clear difference in the catalytic potency between various anionic phospholipids has been found, with phosphatidyl-L-serine (PS) taking a unique position. Jones et al. have shown that PS-containing membranes support thrombin formation at a thousandfold lower concentration than do phosphatidylglycerol (PG)-containing membranes [3]. Rosing et al. demonstrated that membranes containing low surface concentrations of PS, but not PG, would sup-

* Permanent address: a. Fax: +42-2-858-2307; E-mail: hof@jh-inst.cas.cz

¹ This contribution is dedicated to Prof. Dr. F.W. Schneider on the occasion of his 65th birthday.

port thrombin formation even when doped with sufficient positively charged amphiphats to impart a net positive surface potential [4]. On a mechanistic level the preference of the prothrombinase for certain acidic lipids and especially for PS, must reflect either different binding affinities or different catalytic capabilities. Since differences in the binding constants of prothrombin and factor X/Xa to differently composed (e.g. PG- versus PS-containing) membranes [6,7] are far too small to explain the observed differences in catalytic activities of the investigated membrane systems, it has been speculated whether the procoagulant PS induces conformational changes in the substrate factor II and/or the enzyme Xa leading to the PS-specific enhancement in the prothrombinase activity.

Prothrombin fragment 1 (BF1) is the 1–156 N-terminal peptide, which is believed to be the region predominantly responsible for the metal ion and membrane binding properties of prothrombin. Besides small but significant differences in the adsorption rate, it displays basically very similar membrane binding characteristics as the entire protein [8]. The

structure of BF1 is commonly divided into the N-terminal ‘Gla domain’, characterized by 10 γ -carboxyglutamic acid residues (Gla) and a region of disulfide linkages known as the ‘kringle region’. Calcium ions bind (almost) [9] exclusively to the Gla domain and form the native conformation required for membrane binding [10]. Fig. 1 depicts a sketch of the X-ray structure of Ca-BF1 and shows the location of its three tryptophan residues and the seven calcium ions bound to the Gla domain. When examining molecular differences in the binding of the calcium–prothrombin complex to differently composed, negatively charged membrane surfaces, the above mentioned facts lead to the speculation whether such differences can be found in the conformation of membrane-bound Gla domains. Though hints for PS-induced changes in the conformation of other fragments of prothrombin than fragment 1 have been found by differential scanning calorimetry [11–13] and Fourier transform infrared spectroscopy [14], no evidence for the most obvious speculation, a lipid-specific conformational change in the BF1 portion of prothrombin, is reported.

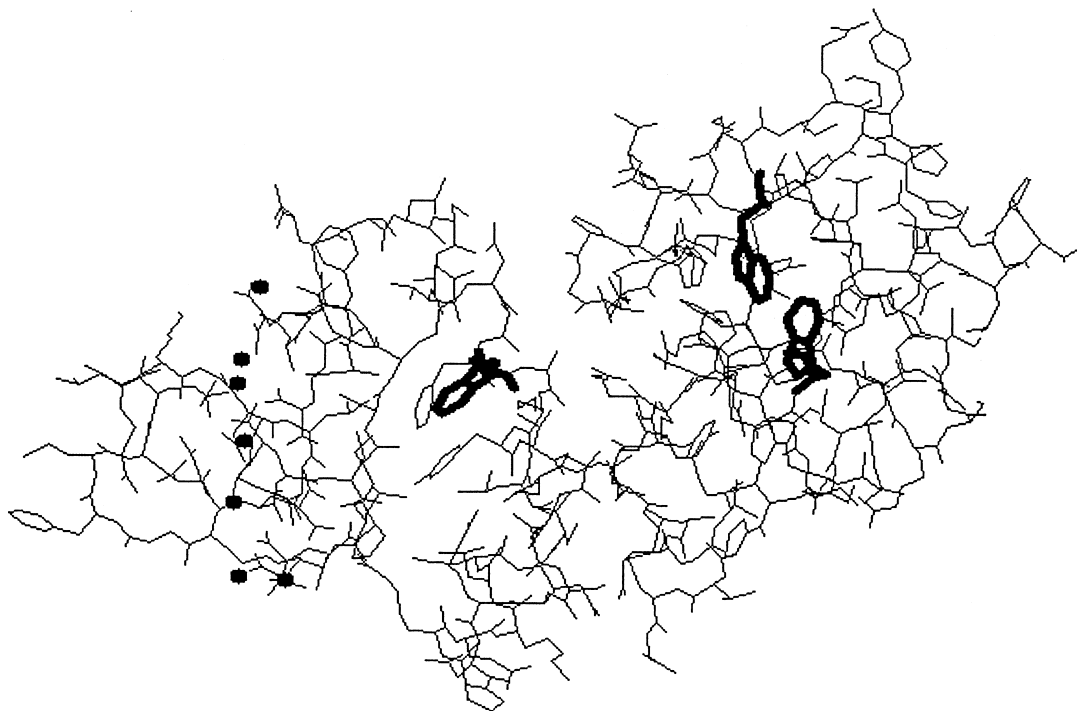


Fig. 1. A depiction of the X-ray structure of Ca-BF1. The right part of the protein is the kringle-domain, where Trp90 and Trp126 are located. The Gla-domain is the left part of the protein, containing Trp42 and seven calcium ions (dots). The coordinates were taken from the Brookhaven Protein Data Bank entries [35] and displayed via Rasmol V2.6 software (Glaxo Wellcome Research Development, Stevenage, UK).

The calcium-induced conformational change in prothrombin, which is essential for membrane binding, can be observed experimentally by circular dichroism [15], by antibody binding experiments [16], differential scanning calorimetric (DSC) studies [11,17], Fourier transform infrared spectroscopy (FTIR) [14] and by intrinsic fluorescence quenching [1,10,18,19]. In a recent work [1] we have presented a detailed study of this conformational change in BF1, taking advantage of the high accuracy of a picosecond fluorescence time-correlated single photon counting experiment. Using this technique, changes in the microenvironment of the three individual tryptophans can be separated from each other without cleaving BF1 into the isolated Gla (containing Trp42) and kringle domains (containing Trp90 and Trp126) or modifying the protein by site-directed mutagenesis. We have shown that addition of calcium ions does not change fluorescence lifetimes and intensities of those components, which have been assigned exclusively to the two kringle tryptophans Trp90 and Trp126 (0.24 ns and 0.68 ns), which argues against a calcium binding site in the kringle domain [9]. On the other hand, we found that the overall fluorescence quenching is due to a static quenching of the Gla-Trp (Trp42) component E (5.1 ns for Ca-BF1) as a consequence of a ground state interaction between Trp42 and the Cys18–Cys23 disulfide bridge. Component D (2.3 ns) comes from the fluorescence of both tryptophan types, with the consequence that the observed decrease in its intensity is smaller than the one detected for component E. It is important to note that an observed decrease in the fluorescence intensity in the 5.1 ns component of 85% is up to magnitudes larger than the calcium-induced changes in the parameters determined by the above listed alternative methods (e.g. for illustration compare Fig. 7 in Ref. [14] with Fig. 6 in Ref. [1]). Component A (40 ps–60 ps) remains due to the limited time resolution of the experiment unassigned.

The high sensitivity of the time-resolved Trp42 fluorescence to conformational changes in the Gla domain was one motivation to re-examine the hypothesis of possible lipid-induced conformational changes in the Gla-domain of prothrombin by picosecond tryptophan fluorescence spectroscopy of BF1. To this end the wavelength-dependent tryptophan

fluorescence decays of Ca-BF1 in the presence of pure phosphatidylcholine (PC) small unilamellar vesicles (SUV) and PC-SUV containing either 25% PS, 25% PG, or 40% PG are characterized, using fluorescence lifetime distribution, conventional multi-exponential, and global analysis.

2. Materials and methods

2.1. Prothrombin fragment 1

Bovine prothrombin fragment 1 was purified as previously described [20–22]. Sodium dodecyl sulfate–polyacrylamide gel electrophoresis indicated homogeneity after silver staining. Concentrations were determined by ultraviolet spectrophotometry at 280 nm ($\epsilon = 1.05 \text{ ml mg}^{-1} \text{ cm}^{-1}$, molecular mass = 23 kDa). Protein solutions were stored in Tris-buffered saline (0.05 M Tris, 0.1 M NaCl; pH 7.4) at -70°C until immediately before use. Fluorescence experiments were carried out at a final concentration of 4 μM BF1 in Tris-buffered saline (0.01 M Tris, 0.1 M NaCl; pH 7.4) at 25°C . BF1 was preincubated with 5 mM CaCl_2 for 30 min before adding it to the vesicle suspensions in Tris buffer containing 5 mM CaCl_2 . The final lipid concentration for all four lipid systems was 1.3 mM.

2.2. Phospholipid vesicles

Aliquots of PS from bovine brain, PG, and PC (both from egg yolk; all from Sigma, St. Louis, MO) in chloroform were combined, dried under a stream of nitrogen to a thin film, redissolved in 1 ml cyclohexane, dried by vacuum centrifugation, and then resuspended to 2 mM with Tris buffer. The lipid mixture was sonicated (Heat Systems Ultrasonics sonicator; Model W-375) for 30 min in an ice bath. Following sonication, the vesicle dispersion was centrifuged for 30 min at $150\,000 \times g$. The top half of the centrifuged vesicle suspension was used within 24 h.

2.3. Light scattering measurements

Equilibrium dissociation constants (K_d) of BF1 binding to small unilamellar vesicles were determined

by light scattering [23]. All solutions except lipid vesicles were passed through a 0.2- μm filter immediately before use. BF1 was preincubated with 5 mM CaCl_2 for 30 min before sequential additions to a magnetically stirred cuvette containing 1.5 ml solutions of 0.05 mg/ml lipid and 5 mM CaCl_2 in Tris buffer (25°C). Scattering intensities were corrected for sample volume increase and scatter of unbound protein. Light scattering at 340 nm was monitored with a SLM 8000 spectrofluorometer (Urbana, IL). The binding isotherms were analyzed essentially by the method of Nelsestuen and Lim [23] using a molecular mass of 23 kDa for BF1 [20]. Apparent outer leaflet phospholipid to protein stoichiometries N/n were calculated from saturation values of the ratio of the molecular mass of the protein-vesicle complex to the molecular mass of the vesicle, $[\text{M}_2/\text{M}_1]_{\text{sat}}$, as described in Ref. [7]. The $[\text{M}_2/\text{M}_1]_{\text{sat}}$ -values were determined from the light scattering isotherms [7]. The values and standard deviations are based on six independent determinations. The K_d -values are $0.9 \pm 0.1 \mu\text{M}$, $0.8 \pm 0.1 \mu\text{M}$, and $2.4 \pm 0.5 \mu\text{M}$ for 25 mol% PS, 40 mol% PG, and 20% PG, respectively. The corresponding N/n -values are 41 ± 8 , 43 ± 9 , and 140 ± 40 for 25 mol% PS, 40 mol% PG, and 20% PG, respectively. The amount of BF1 binding was estimated using equation A13 in the work of Cutsforth et al. [7], which had to be corrected for a typographical error:

$$P_b = P_f \text{PL} / [1.5N/n(K_d + P_f)]$$

P_b and P_f are the concentrations of bound and free protein, respectively. PL is the total phospholipid concentration.

2.4. Fluorescence measurements

Corrected fluorescence spectra were obtained on a SLM 8000 spectrofluorometer (Urbana, IL) using a 'magic angle' configuration. Bandwidths of 2 nm were set for the excitation as well as for the emission. The fluorescence lifetime measurements were performed using a single photon counting technique as described elsewhere [24,25]. The excitation at 295 nm was vertically polarized. The emission was detected after passing through a 'magic angle' polarizer and a J-Y H10 (Instrument SA, Metochen, NJ) monochromator with a 2-nm band pass, on a Hamamatsu

R1645U (Bridgewater, NJ) microchannel plate photomultiplier. Fluorescence decays were collected with 10 000 to 40 000 counts in the peak. The time scales were 14.2, 25.5 and 62.4 ps per channel, 512 channels collected. The instrument response functions (55 ps full width at half maximum) were measured using a light scattering solution of a non-dairy coffee creamer. The fluorescence decays were collected from 300 nm to 420 nm in 5-nm steps. Blank experiments using Tris-buffered saline were performed to exclude distortions by scattered light. The intensity of the scattered light at 300 nm, as well as at the H_2O -Raman band, was negligible.

2.5. Data analysis

For the basic multiexponential analysis a non-linear least-squares iterative reconvolution procedure was used. The program is based on the Marquardt Levenberg algorithm [26] and the optimization includes stray light and time shift [27]. A modified version of the commercially available Edinburgh Analytical Instruments (Edinburgh, UK) global analysis program was employed to simultaneously reconvolve the decays collected at different emission wavelengths. The program also uses the Marquardt Levenberg algorithm. The wavelength-dependent sets of fluorescence decays were analyzed by linking the lifetime values. To characterize the number of classes of fluorescence lifetimes, the Edinburgh Analytical Instruments distribution program was used. In contradiction to analysis using basic multiexponential or continuous distribution models [1,27], no a priori assumption about the distribution shape is made. The fluorescence decay is fit using a sum of hundred lifetime values, which are equally spaced on a logarithmic scale. The best fit is determined by the minimum energy method. The significance and accuracy of the obtained lifetime profiles was tested in an earlier publication [1]. All three programs use reduced χ^2 as a criterion for the goodness of fit evaluation. In the case of the global analysis the mean reduced χ^2 -value (χ^2_{Global}) was used to evaluate the goodness of the fit. The decay-associated spectra (DAS) of Ca-BF1 were determined by combining the time-resolved data with the steady-state emission spectra, as described elsewhere [28]. To determine the emission

maxima, the DAS were fit to log-normal distribution functions [29].

3. Results

For all five investigated systems (Ca-BF1 in Tris buffer as well as Ca-BF1 in the presence of PC-, 25% PS/75% PC-, 40% PG/60% PC-, and 20% PG/80% PC-SUV), the fluorescence decays were recorded at 25 different wavelengths (300 nm to 420 nm). The wavelength-dependent fluorescence behavior was characterized by the distribution of lifetimes method, by conventional multiexponential analysis, and by the global analysis method. The analogous procedures have been described and discussed in detail for apo- and Ca-BF1 [1]. For all five systems investigated in this work, the analysis resulted in a five-exponential decay model, where the five fluorescence lifetimes are wavelength-independent.

3.1. Characterization of the fluorescence decay of Ca-BF1

From the analysis of Ca-BF1 fluorescence decays, five wavelength-independent lifetimes are concluded. The global analysis of the fluorescence decays of the sample preparation investigated in this work yields a χ^2 (Global)-value of 1.19 for a five-exponential analysis. The obtained fluorescence lifetimes 0.05 ± 0.02 ns (component A), 0.24 ± 0.01 ns (B), 0.66 ± 0.02 ns (C), 2.3 ± 0.3 ns (D), and 5.3 ± 0.2 ns (E) are in excellent agreement with the results obtained from a previous sample preparation [1]. The calculated DAS of Ca-BF1 are shown in Fig. 2. The emission maxima of the DAS log-normal fits are 326 nm (component A), 327 nm (B), 334 nm (C), 337 nm (D), and 348 nm (E).

3.2. Fluorescence decays of Ca-BF1 in the presence of PC-SUV

The fluorescence decays of Ca-BF1 in the presence of PC-SUV measured from 300 nm to 420 nm are again characterized by five lifetime components: 0.04 ± 0.02 ns (component A), 0.24 ± 0.02 ns (B), 0.66 ± 0.03 ns (C), 2.4 ± 0.3 ns (D), and 5.4 ± 0.4 ns (E). The obtained χ^2 (Global)-value was 1.28. The pres-

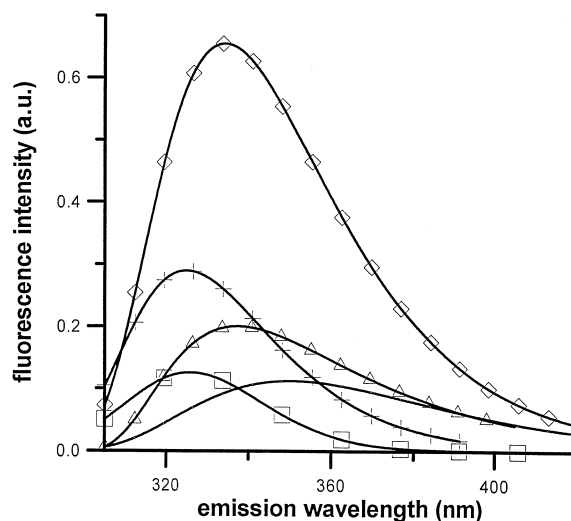


Fig. 2. Decay-associated emission spectra of $4 \mu\text{M}$ Ca-BF1 in Tris buffer ($\lambda_{\text{ex}} = 295$ nm). The fluorescence decay time values are 0.05 ± 0.02 ns (component A, \square), 0.24 ± 0.01 ns (B, $+$), 0.66 ± 0.02 ns (C, \diamond), 2.3 ± 0.3 ns (D, \triangle), and 5.3 ± 0.2 ns (E, no symbol). The emission maxima of the log-normal distribution fits are 326 nm (A), 327 nm (B), 334 nm (C), 337 nm (D), and 348 nm (E). Shown are log-normal distribution fits to the original data.

ence of SUV introduces a high background to the steady-state emission spectrum. Thus, it is more informative to display the wavelength-dependence of the fluorescence by a graph showing the dependence of the corresponding amplitudes on the wavelength (Fig. 3 for components A, B, and C and Fig. 4 for components D and E) rather than by DAS. The amplitude of lifetimes/wavelength dependence of Ca-BF1 in the presence of PC-SUV cannot be distinguished from the one obtained for Ca-BF1 in Tris buffer (data not shown). Obviously, neither non-specific binding to PC-SUV nor the presence of more scattered light changes the apparent, overall fluorescence behavior of Ca-BF1.

3.3. Fluorescence decays of Ca-BF1 in the presence of PS/PC-SUV (25%:75%)

Based on the determined apparent membrane dissociation constant K_d ($0.9 \pm 0.1 \mu\text{M}$) and the phospholipid to protein stoichiometric ratio N/n (41 ± 8), Ca-BF1 ($4 \mu\text{M}$) should have been $> 90\%$ bound to the membrane surface at a lipid concentration of 1.3 mM. Again, the distribution of lifetime analysis (Fig. 5 shows the analysis for $\lambda_{\text{em}} = 400$ nm) as well as the

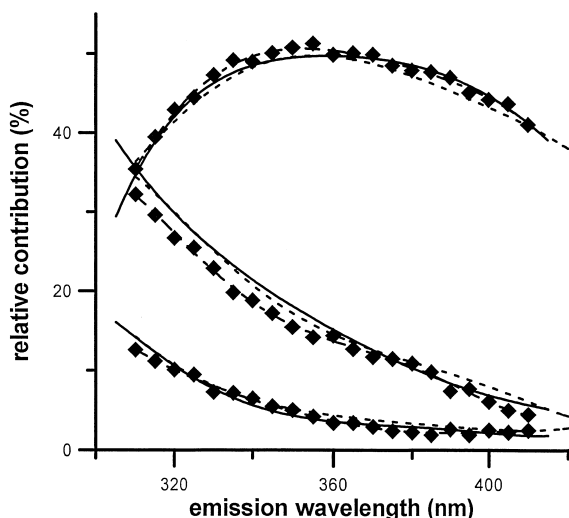


Fig. 3. Amplitude/wavelength dependence of components A, B, C for Ca-BF1 in the presence of PC-SUV (solid line), PS/PC-SUV (25%:75%) (small dashes), and PG/PC-SUV (40%:60%) (large and small dashes). Shown are the polynomial fits (polynomial degree=5). Exemplarily, the original data points are shown for Ca-BF1 in the presence of PG/PC-SUV (40%:60%). Above 320 nm, component C shows the largest contributions and component A the smallest for all three vesicle systems.

global analysis identify the existence of five wavelength-independent lifetimes: 0.04 ± 0.02 ns (component A), 0.23 ± 0.02 ns (B), 0.66 ± 0.03 ns (C), 2.3 ± 0.3 ns (D), and 5.2 ± 0.4 ns (E). The obtained χ^2 (Global)-value was 1.24. Comparison of the ob-

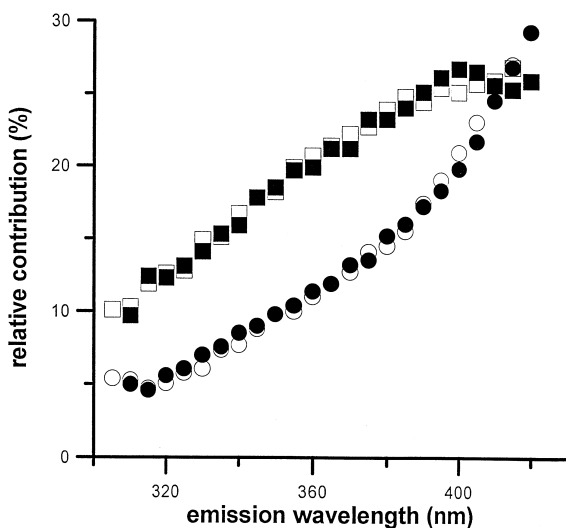


Fig. 4. Amplitude/wavelength dependence of components D (squares) and E (circles) for Ca-BF1 in the presence of PC-SUV (open symbols) and of PS/PC-SUV (25%:75%) (filled symbols). Shown are the original data points.

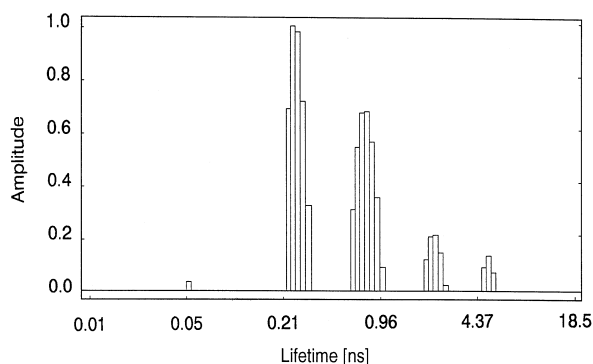


Fig. 5. Amplitude profile of the fluorescence lifetimes distribution of Ca-BF1 in the presence of 1.3 mM 25% PS/75% PC SUV ($\lambda_{\text{ex}} = 295$ nm; $\lambda_{\text{em}} = 400$ nm; $4 \mu\text{M}$ in Tris buffer) resulting from Edinburgh Analytical Instruments distribution analysis of the corresponding fluorescence decay. The resulting mean lifetimes for this measurement are 0.05, 0.26, 0.75, 2.3, and 5.3 ns.

tained lifetimes and the corresponding wavelength dependent amplitudes with those obtained for Ca-BF1 in the presence of PC-SUV (Figs. 3 and 4) shows that specific binding to PS-containing membranes does not change the fluorescence characteristics of Ca-BF1.

3.4. Fluorescence decays of Ca-BF1 in the presence of PG/PC-SUV (40%:60%)

Since the lipid and protein concentrations are identical and the determined binding parameters are very

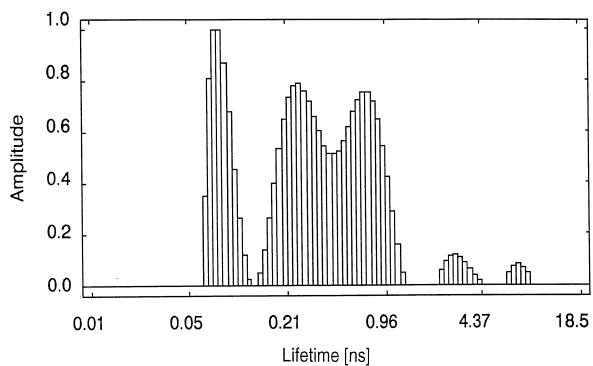


Fig. 6. Amplitude profile of the fluorescence lifetimes distribution of Ca-BF1 in the presence of 1.3 mM PG/PC-SUV (40%:60%) ($\lambda_{\text{ex}} = 295$ nm; $\lambda_{\text{em}} = 360$ nm; 4 mM in Tris buffer) resulting from Edinburgh Analytical Instruments distribution analysis of the corresponding fluorescence decay. The resulting mean lifetimes for this measurement are 0.07, 0.26, 0.70, 3.0, and 7.5 ns.

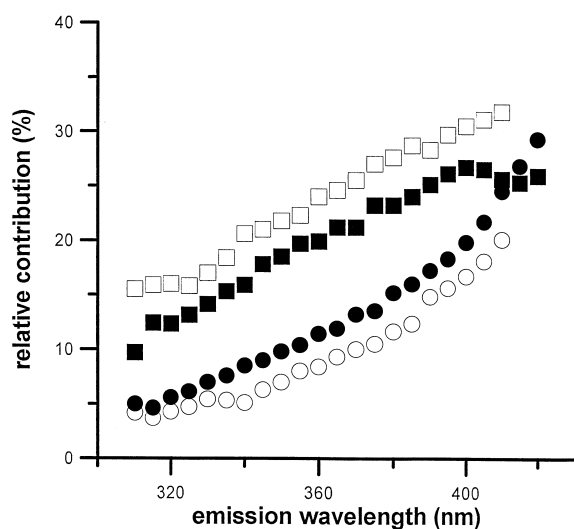


Fig. 7. Amplitude/wavelength dependence of components D (squares) and E (circles) for Ca-BF1 in the presence of PG/PC-SUV (40%:60%) (open symbols) and of PS/PC-SUV (25%:75%) (filled symbols). Shown are the original data points.

similar to the PS-experiment, Ca-BF1 in a concentration of 4 mM should have again been bound at least $>90\%$ to the 40% PG-containing SUV (1.3 mM). As for the PS-containing vesicles, the data analysis yields the existence of five wavelength-independent lifetimes: 0.04 ± 0.02 ns (component A), 0.23 ± 0.03 ns (B), 0.66 ± 0.03 ns (C), 2.8 ± 0.3 ns (D), and 7.5 ± 0.5 ns (E). The obtained $\chi^2(\text{Global})$ -value was 1.32. Exemplarily, the distribution of lifetime analysis for the fluorescence decay recorded at 360 nm is shown in Fig. 6. Apparently, the $>90\%$ binding to PG-containing lipid surfaces prolongs the lifetimes of component E and possibly also component D. Though we observe changes in the amplitudes/wavelength dependence in D and E (Fig. 7), they are too small to allow their extensive physical interpretation. The amplitudes/wavelength dependence in A, B, and C are absolutely identical with those determined in the experiments above (Fig. 3).

3.5. Fluorescence decays of Ca-BF1 in the presence of PG/PC-SUV (20%:80%)

Taking into account the large experimental errors in the binding parameters, the amount of Ca-BF1 (4 μM) binding to 20% PG-containing SUV (1.3 mM) should have been between 40% and 70%. Thus, the fluorescence decay behavior of (roughly) an equimo-

lar mixture of bound and unbound Ca-BF1 was investigated. The purpose of this experiment is to show that the effect of PG-induced increase of the fluorescence lifetimes of components D and E decreases with lower amount of surface binding. The analysis again yielded five lifetime values: 0.03 ± 0.02 ns (component A), 0.23 ± 0.03 ns (B), 0.66 ± 0.03 ns (C), 2.5 ± 0.3 ns (D), and 6.5 ± 0.6 ns (E). The obtained $\chi^2(\text{Global})$ -value was 1.49.

4. Discussion

Before discussing the mechanistic consequences of the observed PG-specific conformational change in the Gla-domain of BF1, the author would like to point out the remarkable reproducibility and significance of the BF1 tryptophan fluorescence: The results obtained from an entirely new sample preparation as well as recorded in the presence of light-scattering PC-SUV are basically identical with those obtained previously [1]. The description of the fluorescence decays in all investigated systems by a decay model with five wavelength-independent lifetimes results from three different analysis procedures (fluorescence lifetimes distribution, Marquardt Levenberg multiexponential analysis, and global analysis). The performed acrylamide quenching studies as well as the calcium induced static quenching not only led to an assignment of components B and C to the krigle-Trp and of the component E to the Trp42, but also confirmed the wavelength-independent five-exponential decay model [1]. Moreover, most recent time-resolved fluorescence investigations of the 1–86 amino acid N-terminus of factor X, which exhibits a Gla domain homologous to prothrombin and contains only a single Trp (Trp41), strongly support the BF1 results and their interpretation [30]: the lifetime values of the Gla-tryptophan (Trp41) in factor X [30] are identical with those found for Trp42 in prothrombin [1], and the calcium-induced conformational change is, as well, paralleled by a static quenching process. This time-resolved fluorescence studies on this second vitamin K-dependent protein [30], together with the conclusiveness of the acrylamide and calcium-induced quenching studies on BF1 [1], lead to an unambiguous interpretation of the decay profiles of BF1 and make further experi-

ments involving site-directed mutagenesis unnecessary. In summary, the components B and C appear to be capable to report conformational changes in the kringle domain, whereas component E gives exclusively information about the fate of the Gla domain. Component D comes from the fluorescence of both Trp-types, and the 40–60 ps component A remains uninterpreted.

As expected, the presence of SUV composed only of the neutral phospholipid does not change the apparent protein conformation. It has been known for a long time that calcium-mediated membrane binding of vitamin K-dependent proteins requires negatively charged phospholipid headgroups, and that, if at all, these proteins only exhibit weak, non-specific binding to PC vesicles [2].

The outstanding specific thrombin-generating activity of PS as compared to other equally charged acidic lipids [3–5,31] has led to the speculation that PS, and not other phospholipids, might trigger specific conformational changes in prothrombin domains and that such changes are connected to the PS-specific enhancement in prothrombinase activity. In this context, the conformation of prothrombin and its isolated fragments has been examined when bound to different catalytic active membrane systems using DSC [11,12] and FTIR spectroscopy [14]. The authors conclude that a PS-induced conformational change occurs rather in the nonmembrane-binding portion of prothrombin (i.e. fragment 2, prethrombin 2), and not in the N-terminal BF1. In this work we have reinvestigated the PS influence on the BF1 conformation, taking advantage of the substantially higher sensitivity of the time-resolved Trp fluorescence (when compared with the cited DSC and FTIR studies) to conformational changes, which is best demonstrated for the calcium-induced conformational change [1]. Based on the determined as well as the literature-referenced binding constants for prothrombin to PS/PC-vesicles [7,32], the used concentrations guarantee a >90% binding to the 25%:75% PS/PC-SUV. The observation that the fluorescence characteristic of BF1 bound to PS containing vesicles is identical with those reported for Ca-BF1 in the presence and absence of PC-SUV is in line with the cited FTIR and DSC investigations. Apparently, the membrane-binding part of calcium-prothrombin remains in its native conformation,

when bound to the highly procoagulant PS-containing membrane surface.

In contrast to the PS results, the tryptophan studies of the ‘PG’-bound BF1 result in the new finding of a lipid-induced conformational change in the Gla-domain, observed by a significant prolongation of lifetime E. At protein/lipid concentrations which ensure that the majority of the protein is bound to the 40%:60% PG/PC-surface, the lifetime of component E shifts from 5.3 to 7.5 ns, when compared with the Ca-BF1 in solution. The prolongation of the Trp42 fluorescence lifetime can be observed as well by an apparent shift of the component D from 2.4 ns to 2.8 ns. On the other hand, as in the case of the binding to PS-containing surfaces, the kringle components B and C remain unchanged. Since component D is due to the fluorescence of Gla and kringle tryptophans, the constant kringle tryptophan fluorescence portion in D might mask the entire magnitude of the lifetime shift in the Gla-portion of component D. Theoretically, a six-exponential decay model should yield the entire shift in the Gla-portion of component D. The fact that the distribution of lifetime analysis never gave more than five peaks for all lifetime data recorded for this work as well as an acceptable χ^2 (Global)-value of 1.32 demonstrate that such a possible sixth component cannot be resolved in the used experimental concept. The observation of a lifetime prolongation in the Trp42 fluorescence due to binding to PG-containing membranes is supported by the studies in the presence of 20%:80% PG/PC-SUV. Here, the fluorescence of roughly an equimolar mixture of ‘free’ and ‘PG-bound’ BF1 is investigated. Again, the limited resolution does not allow the characterization of more than five lifetimes. Thus, the observed component E lifetime value of 6.5 ns is simply the approximate average of lifetime component E in ‘PG-bound’ (7.5 ns) and unbound form (5.3 ns). In summary, it can be concluded that PG influences the fluorescence profile of the Gla-Trp, suggesting a disruption of the Gla-domain conformation. The kringle conformation, on the other hand, appears to be unaffected.

The results presented herein, of course, do not give any information about possible lipid-induced conformational changes in the non-fragment 1 portion of prothrombin. For the N-terminal membrane binding part, however, the comparison between the PS- and

the PG-results leads to the conclusion that the Ca-BF1 already exhibits the 'perfect' conformation for binding and proteolysis and, thus, retains its conformation when bound to PS surfaces. The PG-induced conformational disruption of the Gla domain possibly might affect the protein conformation in the non-fragment 1 part of the protein and/or the lateral diffusion on the membrane surface. Both could be a possible explanation for the lower procoagulant activity of PG when compared with PS. A possible lipid influence on the lateral diffusion of membrane-bound prothrombin is presently under investigation using fluorescence correlation spectroscopy of dye-labeled prothrombin.

One reviewer points out that the experiments have been performed on small unilamellar vesicles, which certainly have a higher curvature than real biological membranes. There are two reasons which make one believe that the curvature of the membrane system used is not crucial for the presented argumentation. First, the conformation of BF1, which is bound to three or four PS or PG molecules [7], should not be affected by the curvature, and second, it is known that lipid assemblies even smaller than SUV are involved in the prothrombin proteolysis [13].

Tryptophan protein studies frequently discuss photophysical reasons for lifetime changes. Certainly, a lifetime value of 7.5 ns is not unusual, but quite large, when compared to other protein tryptophans [28], possibly indicating specific interactions of tryptophan with neighboring functional groups. Considering the following facts, however, a photophysical interpretation appears to be highly speculative in the presented case: (a) since the decay time is generally determined by both, the radiative lifetime and the nonradiative deactivation processes, one has to consider changes in both of them; (b) several functional groups are suspected to prolong tryptophan fluorescence lifetimes [33,34]; (c) the X-ray structure of Ca-BF1 shows several functional groups capable of changing the lifetime in the vicinity of Trp42 [33–35]; (d) the X-ray structure of membrane-bound BF1 could not yet be determined.

It has to be stressed that a correlation between any observed structural differences between the PS and PG bound prothrombin and the different procoagulant activities of these membrane is not fully inescapable. The results presented in this work, however,

strongly suggest to include the role of the Gla domain in the discussion on the molecular reasons for the lipid specificity in the prothrombin proteolysis. This claim is in line with the results of Comfurius et al. [5] indicating that the unique position of PS among the procoagulant phospholipids is correlated with the high affinity of L-serine group (and, e.g., lower affinity of D-serine) for forming a coordination complex in which calcium is chelated by Gla residues of prothrombin and the PS headgroup. Following this, a postulated chelate model for the PS–Ca–Gla interaction [4,5] might lead to an interesting, even if highly speculative, interpretation of the herein presented Trp fluorescence results. The neutral L-serine group of PS appears to be the perfect calcium ligand for the formation of a calcium–chelate complex. In this case the membrane binding to the Ca–Gla domain should be exclusively done via this coordinative Ca–serine binding without any direct binding contribution of the negative charge at the phosphate–oxygen. This mechanistic picture would agree with the fact that only PS is able to support thrombin formation even when imparting a net positive surface potential. In the case of PG, the excellent Ca-ligand serine is substituted by a vicinal diole group, which exhibits a lower coordination affinity to the calcium central atom. Accepting the chelate model, one might speculate that the binding might directly involve the negatively charged phosphate group. The PG–diol group would then be free and could possibly disrupt the Gla domain conformation and/or the Trp42 fluorescence [33,34].

The experimental finding of a PG-specific conformational change in the Gla domain surprisingly finds support by a closer look to the analogous FTIR studies [14]. Though the authors state not having found evidence for conformational change in BF1 induced by binding to both PS-containing as well as to PG-containing membranes, the qualitative comparison of the shape of the shown FTIR spectra (see Fig. 7 in Ref. [14]) might lead to an opposite conclusion. Accepting that the differences in the shown spectra of the Amide I' region of apo- and Ca-BF1 can be interpreted in terms of the above described calcium-induced conformational change in the Gla domain, one is certainly tempted to conclude that PG-containing membranes induce a conformational change in BF1, whereas binding to PS-containing

surfaces does not alter the BF1 conformation (see Fig. 7 in Ref. [14]).

5. Conclusions

The higher sensitivity for conformational changes in BF1 of the picosecond Trp fluorescence when compared with already applied methods made it for the first time possible to detect a lipid-induced conformational change in the Gla domain of prothrombin. Though the differences in the Gla domain conformation of PG bound BF1 compared with the PS bound protein cannot be directly correlated with the different procoagulant activities of these lipids, the results steer the discussion on the molecular reasons for the lipid specificity in the prothrombin proteolysis toward the characterization of the proposed calcium–chelate complex. A possible, and, of course, speculative explanation for the differences in the catalytic activities of the lipids PS and PG could be different lateral diffusion mechanism of the corresponding membrane-bound Gla-domains, which, as shown in this work, show clear conformational differences.

Acknowledgements

The author would like to thank Prof. Graham Fleming, who allowed him to use the instrumentation needed for this work. Further, Prof. Vlastimil Fidler and Dr. Matt Lang are acknowledged for the strong experimental help and Prof. L. Mets for allowing the use his biochemistry lab. The author thanks the Fond der Chemischen Industrie and the Deutsche Forschungsgemeinschaft for habilitation stipends, and the J. Heyrovsky Institute of Physical Chemistry for the internal Grant 5075.

References

- [1] M. Hof, G.R. Fleming, V. Fidler, *Proteins Struct. Func. Genet.* 24 (1996) 485–494.
- [2] J.W. Suttie, C.M. Jackson, *Physiol. Rev.* 57 (1977) 1–70.
- [3] M.E. Jones, B.R. Lentz, F.A. Dombrose, H. Sandberg, *Thromb. Res.* 39 (1985) 711–724.
- [4] J. Rosing, H. Speijer, R.F.A. Zwaal, *Biochemistry* 27 (1988) 8.
- [5] P. Comfurius, E.F. Smeets, G.M. Willems, E.M. Bevers, R.F.A. Zwaal, *Biochemistry* 33 (1994) 10311–10324.
- [6] G.L. Nelsestuen, M. Broderius, *Biochemistry* 16 (1977) 4172–4177.
- [7] G.A. Cutsforth, R.N. Whitaker, J. Hermans, B.R. Lentz, *Biochemistry* 28 (1989) 7453–7459.
- [8] K.H. Pearce, M. Hof, B.R. Lentz, N.L. Thompson, *J. Biol. Chem.* 268 (1993) 22984–22991.
- [9] P. Berkowitz, N.-W. Huh, K.E. Brostrom, M.G. Panek, D.J. Weber, A. Tulinsky, L.G. Pedersen, R.G. Hiskey, *J. Biol. Chem.* 267 (1992) 4570–4576.
- [10] G.L. Nelsestuen, *J. Mol. Biol.* 251 (1976) 5648–5656.
- [11] B.R. Lentz, J.R. Wu, A.M. Sorrentiono, J.N. Carleton, *Biophys. J.* 60 (1991) 942–961.
- [12] B.R. Lentz, C.M. Zhou, J.R. Wu, *Biochemistry* 33 (1994) 5460–5468.
- [13] V. Koppaka, J. Wang, M. Banerjee, B.R. Lentz, *Biochemistry* 35 (1996) 7482–7491.
- [14] J.R. Wu, B.R. Lentz, *Biophys. J.* 60 (1991) 70–80.
- [15] J.W. Bloom, K.G. Mann, *Biochemistry* 17 (1978) 4430–4438.
- [16] M. Borowski, B.C. Furie, S. Bauminger, B. Furie, *J. Biol. Chem.* 261 (1986) 14969–14975.
- [17] V.A. Plopis, D.K. Strickland, F.J. Castellino, *Biochemistry* 20 (1981) 15–21.
- [18] F.G. Prendergast, K.G. Mann, *J. Biol. Chem.* 252 (1977) 840–850.
- [19] H.C. Marsh, M.E. Scott, R.G. Hiskey, K.A. Koehler, *Biochem. J.* 183 (1979) 513–517.
- [20] K.G. Mann, *Methods Enzymol.* 45 (1976) 123–156.
- [21] J.S. Pollock, A.J. Shepard, D.J. Weber, D.L. Olson, D.G. Klapper, L.G. Pedersen, R.G. Hiskey, *J. Biol. Chem.* 263 (1988) 14216–14223.
- [22] S.W. Tendian, B.R. Lentz, *Biochemistry* 29 (1990) 6720–6729.
- [23] G.L. Nelsestuen, T.K. Lim, *Biochemistry* 16 (1977) 4164–4171.
- [24] M.C. Chang, S.H. Coutney, A.J. Cross, R.J. Gulotty, J.W. Petrich, G.R. Fleming, *Anal. Instrum.* 14 (1985) 433–464.
- [25] J.E. Hansen, J.W. Longworth, G.R. Fleming, *Biochemistry* 29 (1990) 7329–7338.
- [26] D.W. Marquardt, *J. Soc. Ind. Appl. Math.* 11 (1963) 431–441.
- [27] M. Hof, J. Schleicher, F.W. Schneider, *Ber. Bunsenges. Phys. Chem.* 93 (1989) 1377–1381.
- [28] M.R. Eftink, in: C.H. Suelter (Ed.), *Protein Structure Determination: Methods of Biochemical Analysis*, vol. 35, John Wiley, New York, 1991, pp. 127–205.
- [29] D.B. Siano, D.E. Metzler, *J. Chem. Phys.* 51 (1969) 1856–1861.
- [30] A. Häfner, F. Merola, G. Duportail R. Hutterer, F.W. Schneider, M. Hof, in preparation.
- [31] G. Pei, D.D. Powers, B.R. Lentz, *J. Biol. Chem.* 268 (1993) 3226.

- [32] K.H. Pearce, Ph.D. Thesis, University of North Carolina at Chapel Hill, USA, 1993.
- [33] D.L. Harris, B.S. Hudson, *Biochemistry* 29 (1990) 5276–5285.
- [34] S. Kim, F.N. Chowdhury, W. Stryjewski, E.S. Younathan, P.S. Russo, M.D. Barkley, *Biophys. J.* 65 (1993) 215–226.
- [35] M. Soriano-Garcia, C.H. Park, A. Tulinsky, K.G. Ravichandran, E. Skrzypczak-Jankun, *Biochemistry* 28 (1989) 6805–6810.